Received: 1 July 2023 | Revised: 29 August 2023 | Accepted: 29 August 2023

DOI: 10.1002/pamm.202300219

RESEARCH ARTICLE

Mixed-integer NMPC for real-time supervisory energy management control in residential buildings

Dimitri Bitner[1] | **Artyom Burda**[1,2] | **Martin Grotjahn**[1] | **Christian Kirches**[2] | **Axel Schild**[3] | **Bennet Luck**[3]

[1]Institute of Engineering Design, Mechatronics and Electromobility, Hannover University of Applied Sciences and Arts, Ricklinger Stadtweg 120, Hannover, Germany

[2]Institute for Mathematical Optimization, Technische Universität Carolo-Wilhelmina zu Braunschweig, Universitätsplatz 2, Braunschweig, Germany

[3]IAV GmbH, Carnotstraße 1, Berlin, Germany

Correspondence
Dimitri Bitner, Institute of Engineering Design, Mechatronics and Electromobility, Hannover University of Applied Sciences and Arts, Ricklinger Stadtweg 120, 30459 Hannover, Germany.
Email: dimitri.bitner@hs-hannover.de

Funding information
DFG, Grant/Award Numbers: Ki 1839/1-2, Ki 1839/3-1; BMBF, Grant/Award Number: 05M20MBA-LEOPLAN; BMWK, Grant/Award Number: 03EN1007A-EEBF

Abstract

In recent years, building energy supply and distribution systems have become more complex, with an increasing number of energy generators, stores, flows, and possible combinations of operating modes. This poses challenges for supervisory control, especially when balancing the conflicting goals of maximizing comfort while minimizing costs and emissions to contribute to global climate protection objectives. Mixed-integer nonlinear model predictive control is a promising approach for intelligent real-time control that is able to properly address the specific characteristics and restrictions of building energy systems. We present a strategy that utilizes a decomposition approach, combining partial outer convexification with the Switch-Cost Aware Rounding procedure to handle switching behavior and operating time constraints of building components in real-time. The efficacy is demonstrated through practical applications in a single-family home with a combined heat and power unit and in a multi-family apartment complex with 18 residential units. Simulation studies show high correspondence to globally optimal solutions with significant cost savings potential of around 19%.

1 | INTRODUCTION

Energy management systems provide a cost-effective way to directly reduce energy consumption in buildings. According to [1], the implementation of intelligent building automation has the potential to achieve energy savings of up to 30%, leading to a significant reduction in CO_2 emissions. The latter point is of significant importance due to global climate protection goals implemented through a society-wide transformation to sustainable energy production; compare, for example, [2].

A promising candidate for an intelligent real-time supervisory control system is a model predictive control (MPC) strategy. Of particular interest is nonlinear MPC (NMPC), which can be directly applied to nonlinear multi-dimensional systems, as they occur in the building sector. The method has already been successfully applied in various studies for different building configurations and components, such as absorption chillers with energy savings of 31.1% [3], domestic micro-grids with 10% savings [4], or temperature controls with around 17% savings [5] compared to conventional control methods.

Here we present an advanced control strategy, mixed-integer NMPC (MI-NMPC), in order to consider integer controls and restrictions on typical building technology components without considerable problem reformulations. The strategy utilizes a decomposition approach, where an approximation of the optimal solution is determined by a combination of a partial outer convexification reformulation and an integer control reconstruction procedure to achieve real-time capability. We take into account the switching behavior of the building components along with admissible operating time constraints, so-called dwell times. The work of Bürger et al. [6] also presents a method for addressing the constraints imposed by dwell-times in a solar-driven climate system. However, this method combines the use of MI-NMPC with a binary approximation problem solver called *pycombina* [7], which can be computationally expensive. In contrast, our approach utilizes the advanced and efficient cutting-edge switch-cost aware rounding (SCARP) procedure.

We shortly summarize the results of a simulation study for the energy system of a single-family house performed in [8]. The real-time performance and the resulting quality of the solution have been proved by their high correspondence to the globally optimal solution calculated by the computationally costly dynamic programming (DP) method. Moreover, we describe in detail the application and corresponding results of the strategy to a more complex optimization task with multiple degrees of freedom resulting from a multi-family house with 18 residential units.

The article is structured as follows. First, we describe the workflow for solving general mixed-integer optimal control problems (MIOCPs), as they arise in the energy management of buildings. Next, we present the application to the single-family house from [8, 9], and then provide a more detailed description of the optimal control problem for the multi-family residential and provide initial numerical results using the proposed solution method. The article concludes with a summary of findings and an outlook on future work.

2 | SOLUTION APPROACH

We first explain the problem formulation typically resulting from building energy applications, followed by the workflow for solving the problem. It consists of convexification and relaxation of the original problem, followed by a rounding strategy to generate a binary solution for the switching control variables, and finally, a post-processing step to avoid possible constraint violations. The solution strategy is described here in a general and condensed form. For a detailed description, refer to [8].

2.1 | Problem formulation

The primary objectives of managing an energy supply system involve the dual focus of minimizing energy expenses and maintaining a consistent provision of the necessary energy. This objective is typically addressed through a multi-objective approach that aims to optimize economic control by assessing the cumulative operating costs as the primary objective function. However, the discrete on/off attributes of the system components, combined with their ability to operate within a continuous range, introduce a complex challenge in the form of a MIOCP

$$\min_{\boldsymbol{x}(\cdot),\boldsymbol{u}(\cdot),\boldsymbol{v}(\cdot)} \int_{t_0}^{t_\mathrm{f}} L(\boldsymbol{x}(t),\boldsymbol{u}(t),\boldsymbol{v}(t))\,\mathrm{d}t \tag{1a}$$

$$[-2pt]\text{s.t. } \dot{\boldsymbol{x}}(t) = f(\boldsymbol{x}(t),\boldsymbol{u}(t),\boldsymbol{v}(t)), \qquad t \in [t_0,t_\mathrm{f}] \tag{1b}$$

$$\boldsymbol{x}(t_0) = \hat{\boldsymbol{x}}_0, \tag{1c}$$

$$\boldsymbol{x}(t) \in [\boldsymbol{x}_{\min},\boldsymbol{x}_{\max}],\ \boldsymbol{u}(t) \in [\boldsymbol{u}_{\min},\boldsymbol{u}_{\max}],\ \boldsymbol{v}(t) \in \{0,1\}^{n^v}, t \in [t_0,t_\mathrm{f}] \tag{1d}$$

$$\boldsymbol{0} \le \boldsymbol{c}(\boldsymbol{x}(t),\boldsymbol{u}(t),\boldsymbol{v}(t)), t \in [t_0,t_\mathrm{f}] \tag{1e}$$

where $\boldsymbol{x}$ represents the system's states, including the temperatures and states of charge of electrical and thermal storage. By $\boldsymbol{u}$ and $\boldsymbol{v}$ we denote vectors of continuous and binary control variables, respectively, for the generators and storage charging/discharging (when applicable). We have constraint (1b) to capture the system dynamics, along with (1d) to define

the bounds for states and inputs. Additionally, there are arbitrary inequality constraints (1e) that ensure the appropriate assignment of electricity prices for feed-in and purchase, among other conditions.

2.2 | Mixed-integer NMPC strategy

The system control problem presented in Equation (1) exhibits typical characteristics of an MIOCP. The binary control functions $\boldsymbol{v}$ are typically involved in a nonlinear and non-convex manner in Equations (1a) and (1b). As a result, after discretization in time, the problem becomes an NP-hard non-convex mixed-integer nonlinear programming (MINLP) problem, compare [10].

To address this challenge, we employ a partial outer convexification approach as outlined in [11] for Equations (1a) and (1b) and in [12] for Equation (1e). This approach leads to a transformed MIOCP formulation that becomes linear and convex when considering the relaxed indicator controls $\boldsymbol{\alpha}$. Consequently, the resulting problem can be regarded as a continuous optimal control problem (OCP)

$$\min_{\boldsymbol{x}(\cdot),\boldsymbol{u}(\cdot),\boldsymbol{\alpha}(\cdot)} \sum_{i=1}^{2^{n^v}} \int_{t_0}^{t_f} \alpha_i(t) L(\boldsymbol{x}(t), \boldsymbol{u}(t), \boldsymbol{w}_i)\, \mathrm{d}t \tag{2a}$$

$$[-2pt]\text{s.t. } \dot{\boldsymbol{x}}(t) = \sum_{i=1}^{2^{n^v}} \alpha_i(t) f(\boldsymbol{x}(t), \boldsymbol{u}(t), \boldsymbol{w}_i), \qquad t \in [t_0, t_f] \tag{2b}$$

$$\boldsymbol{x}(t_0) = \hat{\boldsymbol{x}}_0, \tag{2c}$$

$$\boldsymbol{x}(t) \in [\boldsymbol{x}_{\min}, \boldsymbol{x}_{\max}],\ \boldsymbol{u}(t) \in [\boldsymbol{u}_{\min}, \boldsymbol{u}_{\max}], t \in [t_0, t_f] \tag{2d}$$

$$\boldsymbol{\alpha}(t) \in [0,1]^{2^{n^v}},\ 1 = \sum_{i=1}^{2^{n^v}} \alpha_i(t), t \in [t_0, t_f] \tag{2e}$$

$$\mathbf{0} \leq \alpha_i(t) \boldsymbol{c}(\boldsymbol{x}(t), \boldsymbol{u}(t), \boldsymbol{w}_i), \forall i \in \{1, \dots, 2^{n^v}\},\ t \in [t_0, t_f] \tag{2f}$$

with α_i as a binary indicator function (sometimes called a one-hot encoding) for each possible choice of $\boldsymbol{v}(t) = \boldsymbol{w}_i \in \{0,1\}^{n^v}$. Even though those are formally 2^{n^v}, that is exponentially many, in practical applications a large number of choices typically encodes binary control actions that are not sensible and can be removed from the problem (2) a priori. To solve the problem (2), well-established techniques for direct optimal control exist, such as direct multiple shooting [13] or direct collocation [14].

To determine an appropriate binary control $\boldsymbol{\omega}^N$ from an optimal solution $(\boldsymbol{x}^N, \boldsymbol{u}^N, \boldsymbol{\alpha}^N)$ that was obtained by discretizing (2) into N time elements, we utilize the novel SCARP procedure using a shortest-path approach, initially introduced in [15, 16] and successfully applied in [8]. One of the limitations of SCARP is the inability to consider disturbances to the system's states $x(t)$ when computing the binary solution from a relaxed optimal one. Consequently, applying a rounded solution can lead to violations of the state bounds or path constraints (2d) formulated in the original oOCP. Therefore, a post-processing step is performed before applying the solution to the process. We solve problem (2) again, fixing the SCARP solution and making use of the remaining continuous control degrees of freedom to satisfy the constraints.

3 | APPLICATION TO ENERGY SUPPLY SYSTEM OF SINGLE-FAMILY HOUSE

The energy supply system for the single-family house includes a gas-driven modulating micro combined heat and power (CHP) unit, a condensing boiler as a backup heater, and a buffer storage tank (see Figure 1). Thermal energy generated by the CHP unit is stored in the buffer tank and used for heating and domestic hot water. The electricity generated by the CHP unit is consumed within the house, with excess energy being fed into the grid and electrical energy shortages being covered by the grid. Thus, the system has different energy sources with nonlinear efficiency curves and variable costs. Moreover, the CHP unit generates both electricity and heat simultaneously, but their demands may not always align, and the storage capacity is limited.

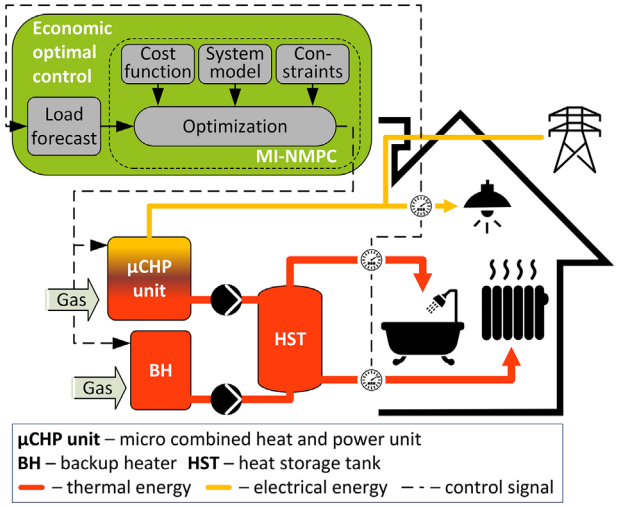

FIGURE 1 Energy supply system of single-family house consisting of micro combined heat and power unit (µCHP unit), backup heater (BH) and heat storage tank (HST).

This leads to a multi-objective economic OCP with binary and continuous control variables for each generator and one state variable representing the thermal energy in the buffer storage. The OCP also incorporates a dwell-time requirement, ensuring that the CHP unit operates for a minimum duration of 60 min for durability reasons. For a comprehensive system and problem description, refer to [8, 9].

To achieve the objective of minimizing total operating costs, the DP approach as well as the proposed strategy (Res) utilize information on future energy demands. They adjust the operating hours of the CHP unit to coincide with peak electrical load periods whenever possible (see Figure 2). The buffer storage capacity is fully utilized to bridge periods of low electrical consumption. These approaches maximize in-house electricity generation while minimizing uneconomical feed-in. Additionally, the thermal energy requirements are consistently met, ensuring that the storage limits of 13.5 and 50 kWh are not exceeded. In contrast, the conventional heat-led control strategy (SoA) primarily relies on the level of the storage tank and the outdoor temperature. Predefined time intervals for low, medium, or high production are used to determine the desired storage tank level. This results in maintaining a higher overall level in the storage tank. However, since the future demand is not known in advance, the controller always aims to preserve sufficient thermal energy for high consumption periods. The boiler functions as a backup heater and is only activated during periods of high thermal demand on extremely cold days. In the analyzed timeframe, there is no need for support from the backup heater at any point. In total, the optimizer using DP achieves cost savings of 18.9% compared to the SoA strategy for a simulated period

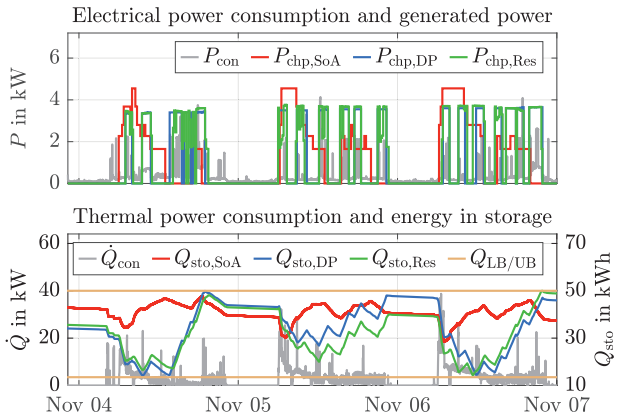

FIGURE 2 Characteristics of the power supply system - power consumption (P_{con} and $\dot{Q}_{con}$) and generated electrical power (P) and thermal energy in storage Q_{sto} with heat-led control strategy (SoA), dynamic programming approach (DP), and proposed strategy (Res); lower (LB) and upper (UB) heat storage limits.

of one week, however with a high computational effort. By providing an approximated optimal solution in a significantly shorter time, the proposed real-time capable approach still achieves cost savings of 16.4%.

4 | APPLICATION TO ENERGY SUPPLY SYSTEM OF MULTI-FAMILY RESIDENTIAL

4.1 | System description and problem definition

In this section, we consider a more complex energy supply system that is widespread in modern multifamily residentials and is actually deployed in a real building. As schematically illustrated in Figure 3, it consists of two thermal energy generators: a heat pump and a gas boiler. The generated energy is then, in order to follow the requirements on different temperature levels, distributed among two heat storage tanks, one dedicated only to domestic hot water and another to hydronic heating. The electrical energy, required for the operation of the heat pump can be obtained from the battery storage which is charged through the installed photovoltaic unit or purchased from the grid. The excesses of the generated electrical energy can be stored in the battery storage or delivered to the other power units within the energy supply system (gas boiler, pumps, valves, etc.). Thus, the system consists of energy units and flows whose dynamics is highly nonlinear along with a large number of disturbances both at the consumption and generation sides. It is obvious that the complexity of this system is much higher in comparison to the system from Section 4, however, the overall concept and objectives are absolutely the same. Therefore, we implement a similar modeling strategy and the very same MI-NMPC-based solution approach.

4.2 | Modeling approach

We want to accurately follow the state of the heat storage tanks using rather simple energy balance equations. The high dynamics of the domestic hot water demand is met by the buffer storage tank and therefore causes unnecessary complexity for the optimizer. Hence, the high peaks of the domestic hot water demand are smoothed and we do a similar procedure of encapsulation of both storages for the domestic hot water and hydronic heating here. As a consequence the dynamics of one cumulative heat storage tank has to be described.

We start with the description of the energy generators and then will follow the energy flows to the heat storage tank. Similar to [9], we introduce an integer control to represent the state of an energy unit and a continuous input for its power modulation. Thus, the boiler heating power of the gas reads

$$\mathring{Q}_{\mathrm{g,boi}}(t) = u_{\mathrm{boi}}(t) v_{\mathrm{boi}}(t), \tag{3}$$

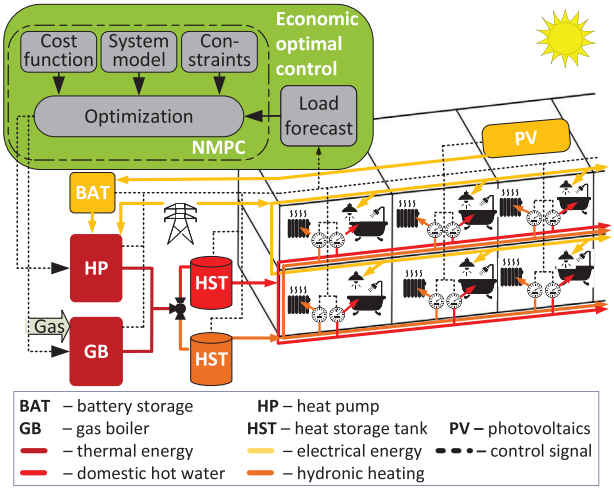

FIGURE 3 Energy supply system of multi-family residential consisting of heat pump (HP), gas boiler (GB), photovoltaic system (PV), heat storage tank (HST) and battery storage (BAT).

with the modulated input power $u_{\mathrm{boi}} \in [5, 40]$ (kW) and integer input $v_{\mathrm{boi}} \in \{0, 1\}$. The boiler is well-insulated in practice and therefore, omitting the losses to the ambient, its resulting thermal output power is: $\mathring{Q}_{\mathrm{boi}}(t) = \eta_{\mathrm{boi}}\mathring{Q}_{\mathrm{g,boi}}(t)$. Here, the boiler efficiency η_{boi} is selected constant and along with all the necessary parameters given in Table 1. Similarly, the electrical output power of the heat pump is given by $P_{\mathrm{HP,el}}(t) = u_{\mathrm{HP}}(t)v_{\mathrm{HP}}(t)$, with $u_{\mathrm{HP}} \in [0.4, 2.5]$ (kW) and the resulting thermal output power is represented by $\mathring{Q}_{\mathrm{HP}}(t) = \eta_{\mathrm{HP}}(t)\mathring{Q}_{\mathrm{HP,el}}(t)$. Unlike for the gas boiler, where its efficiency does not fluctuate a lot depending on the flow and return temperature, the heat pump coefficient of performance (COP) $\eta_{\mathrm{HP}}(t)$ highly depends also on the ambient temperature. Therefore, accurate calculation of the efficiency here is crucial and for the current scenario is performed by means of a spline function, based on the efficiency curves from the heat pump documentation.

We divide the storage tank into three compartments since its charging and discharging is taking place in the pipes at different height with $\theta_{1,2,3}(t)$ representing the water temperatures in the corresponding compartments. Due to the consideration of only one storage and its direct connection to the heat pump, the water flows out of the storage $\mathring{m}_{\mathrm{sto}}(t)$ is equivalent to the water flow into the heat pump $\mathring{m}_{\mathrm{HP}}(t)$. The water pipes connecting heat storage with the heat pump and the space heating station are located in compartment three of the storage tank and therefore the water temperatures there are considered equal $\theta_{\mathrm{sto,out}}(t) = \theta_{\mathrm{sto},3}(t) = \theta_{\mathrm{HP,in}}(t)$. The flow temperature of the heat pump is based on its resulting heating power output:

$$\theta_{\mathrm{HP,out}}(t) = v_{\mathrm{HP}}(t)\mathbf{S}(\theta_{\mathrm{amb}}, \theta_{\mathrm{HP,in}}, \theta_{\mathrm{HP,out}})P_{\mathrm{HP,el}}(t)\big/(c_{\mathrm{w}}\mathring{m}_{\mathrm{sto}}(t)) + \theta_{\mathrm{HP,in}}(t), \tag{4}$$

where $\mathbf{S}(\cdot)$ is the heat pump efficiency spline function based on the efficiency curves from the documentation. Actual measurements of the ambient temperature $\theta_{\mathrm{amb}}(t)$ are used first and later will be replaced by an external forecast model. If additional heating is required, it is achieved with the help of the gas boiler and the resulting inlet temperature of the storage reads

$$\theta_{\mathrm{sto,in}}(t) = v_{\mathrm{boi}}(t)\mathring{Q}_{\mathrm{boi}}(t)\big/(c_{\mathrm{w}}\mathring{m}_{\mathrm{sto}}(t)) + \theta_{\mathrm{HP,out}}(t). \tag{5}$$

The heat storage discharge takes place from compartment 1. The temperature after the heating circuit then can be derived by

$$\theta_{\mathrm{SH,out}}(t) = \theta_{\mathrm{sto},1}(t) - P_{\mathrm{SH}}(t)\big/(c_{\mathrm{w}}\mathring{m}_{\mathrm{SH}}(t)), \tag{6}$$

with P_{SH} as a space heating demand and $\mathring{m}_{\mathrm{SH}}$ as the space heating inlet water flow. The system's thermal consumption is treated as a time-varying parameter and for the initial simulations is provided by the measurements. However, an accurate heat demand forecast model is to be used later, when the deployment of the controller takes place.

In order to describe convective flows in the storage, we require a function with a switching behavior, dependent on the temperatures of the compartments. This is however highly undesirable for derivative-based optimization. Therefore, we utilize a smoothing function S to achieve a smoothing transition between the convective flow directions. Thus, the resulting convective flow between compartments 1 and 2 is: $\mathring{Q}_{12}(t) = S(\mathring{m}_{\mathrm{SH}}(t) - \mathring{m}_{\mathrm{sto}}(t), \theta_{\mathrm{sto},2}(t), \theta_{\mathrm{sto},1}(t))$, for compartments 2 and 3: $\mathring{Q}_23(t) = S(\mathring{m}_{\mathrm{sto}}(t) - \mathring{m}_{\mathrm{SH}}(t), \theta_{\mathrm{sto},2}(t), \theta_{\mathrm{sto},3}(t))$ and overall convective flow: $\mathring{Q}_123(t) = S(\mathring{m}_{\mathrm{sto}}(t) - \mathring{m}_{\mathrm{SH}}(t), \theta_{\mathrm{sto},1}(t) - \theta_{\mathrm{sto},2}(t), \theta_{\mathrm{sto},2}(t) - \theta_{\mathrm{sto},3}(t))$.

The resulting dynamics for the compartment temperatures are then obtained as follows

$$\dot{\theta}_{\mathrm{sto},1}(t) = \left[\mathring{m}_{\mathrm{sto}}(t)\theta_{\mathrm{sto,in}}(t) - \mathring{m}_{\mathrm{SH}}(t)\theta_{\mathrm{sto},1}(t) + \mathring{Q}_12(t) + (-\beta_{\mathrm{sto}}(\theta_{\mathrm{sto},1}(t) - \theta_{\mathrm{amb}}) - A_{\mathrm{sto}}\alpha_{\mathrm{w}}(\theta_{\mathrm{sto},1}(t) - \theta_{\mathrm{sto},2}(t)))/c_{\mathrm{w}}\right]\Big/\frac{m_{\mathrm{sto}}}{3}, \tag{7}$$

$$\dot{\theta}_{\mathrm{sto},2}(t) = \left[\mathring{Q}_123(t) + (-\beta_{\mathrm{sto}}(\theta_{\mathrm{sto},2}(t) - \theta_{\mathrm{amb}} + A_{\mathrm{sto}}\alpha_{\mathrm{w}}(\theta_{\mathrm{sto},1}(t) - \theta_{\mathrm{sto},2}(t)) - A_{\mathrm{sto}}\alpha_{\mathrm{w}}(\theta_{\mathrm{sto},2}(t) - \theta_{\mathrm{sto},3}(t)))/c_{\mathrm{w}}\right]\Big/\frac{m_{\mathrm{sto}}}{3}, \tag{8}$$

$$\dot{\theta}_{\mathrm{sto},3}(t) = \left[\mathring{m}_{\mathrm{SH}}(t)\theta_{\mathrm{SH,out}}(t) - \mathring{m}_{\mathrm{sto}}(t)\theta_{\mathrm{sto},3}(t) + \mathring{Q}_23(t) + (-\beta_{\mathrm{sto}}(\theta_{\mathrm{sto},3}(t) - \theta_{\mathrm{amb}}) + A_{\mathrm{sto}}\alpha_{\mathrm{w}}(\theta_{\mathrm{sto},2}(t) - \theta_{\mathrm{sto},3}(t)))/c_{\mathrm{w}}\right]\Big/\frac{m_{\mathrm{sto}}}{3}. \tag{9}$$

Now, on the side of electrical energy, we first calculate the battery charge from the photovoltaic system (PV)

$$P_{\mathrm{bat,in}}(t) = A_{\mathrm{PV}}\eta_{\mathrm{PV}}I_{\mathrm{sol}}(t) - P_{\mathrm{PV,der}}(t), \tag{10}$$

where $I_{\mathrm{sol}}(t)$ is the time-varying solar irradiance measurement or prediction data. $P_{\mathrm{PV,der}}(t)$ corresponds to the control input for the electric power derating from the PV. Since the PV system and the battery are not able to cover the full electrical

TABLE 1 Model parameters.

Name	c_w	α_w	A_{sto}	β_{sto}	E_{bat}	η_{boi}	A_{PV}	η_{PV}	m_{HP}	m_{SH}	m_{sto}
Description	Water heat capacity	Water heat conductivity	Storage area	Storage ambient loss coefficient	Electrical battery size	Boiler efficiency	Photovoltaic area	Photovoltaic efficiency	Heat pump mass flow	Space heating mass flow	Heat storage capacity
Value	4180	0.5562	0.56	0.0012	5.12	0.958	40.2402	0.1228	0.9	0.2	3000
Unit	kJ/kgK	W/mK	m^2	W/K	kWh	-	m^2	-	kg/s	kg/s	kg

demand of the energy generators, we have to consider the electricity purchases from the grid. The corresponding power reads

$$P_{\mathrm{grd}}(t) = \upsilon_{\mathrm{HP}}(t) P_{\mathrm{HP,el}}(t) + \upsilon_{\mathrm{boi}}(t) P_{\mathrm{boi,el}}(t) - P_{\mathrm{bat,out}}(t), \tag{11}$$

where $P_{\mathrm{boi,el}}(t)$ is the electrical power of the boiler and is assumed to be directly proportional to its gas power output $P_{\mathrm{boi,el}}(t) = \eta_{\mathrm{boi,el}} P_{\mathrm{boi,gas}}(t)$. The dynamics of the battery state of charge can then be derived from

$$\dot{SOC}_{\mathrm{bat}}(t) = \left(P_{\mathrm{bat,in}}(t) - P_{\mathrm{bat,out}}(t)\right) / E_{\mathrm{bat}}. \tag{12}$$

In the end, we deal with the system with 4 state variables $\boldsymbol{x}^T = (\theta_{\mathrm{sto},1}, \theta_{\mathrm{sto},2}, \theta_{\mathrm{sto},3}, SOC_{\mathrm{bat}})$ and an input vector with six components $\boldsymbol{u}^T = (\upsilon_{\mathrm{HP}}, \mathring{m}_{\mathrm{HP}}, \upsilon_{\mathrm{boi}}, u_{\mathrm{boi}}, P_{\mathrm{bat,out}}, P_{\mathrm{PV,der}})$.

4.3 | Problem formulation

Having a similar goal to the single-family house of minimizing the energy expenses, we formulate the objective term

$$L(t, \boldsymbol{u}(t), \boldsymbol{v}(t)) = \upsilon_{\mathrm{boi}}(t) \mathring{Q}_{\mathrm{g,boi}}(t) p_{\mathrm{gas}} + P_{\mathrm{grd}}(t) p_{\mathrm{el}}, \tag{13}$$

representing the total costs spent on gas and electricity purchases with p_{gas} and p_{el} as prices for the gas and electricity purchases, respectively. In order to ensure the safe operation of the system we introduce several trivial path box constraints on temperature levels in the storage $\theta_{1,2,3}$ and hardware constraint on the heat pump maximum temperature difference $\theta_{\mathrm{HP,out}} - \theta_{\mathrm{HP,in}}$. A terminal constraint to keep the heat storage and the battery state on certain levels at the end of the prediction horizon is also imposed. The resulting system control problem is a MIOCP of the same form as in [8] but with a more-dimensional and complex model described above. Therefore, we omit the interim problem formulation here. Following the convexification and relaxation procedures from Section 2, we introduce one-hot encoding similar to [8] here $\boldsymbol{\omega}(t) : \mathbb{S}^4 \to \Omega := \{0,1\}^2$, but for the integer inputs for the boiler and the heat pump on/off states. Relaxation procedure then replaces $\boldsymbol{\omega} \in \{0,1\}^4$ with $\boldsymbol{\alpha} \in [0,1]^4$. Consequently, the continuous OCP of the form from Equation (2) with $n^{\upsilon} = 2$ is solved. In the current formulation, we choose a rather large sampling time of 15 min and therefore we can omit the minimum operation time constraints for the energy generators.

4.4 | Numerical results

We provide and investigate the simulation results for the prediction horizon of 24 h with a sampling time of 900 s. The continuous OCP is discretized and parametrized by means of the multiple-shooting method. It results in an nonlinear program that is solved with an sequential quadratic programming (SQP) method in combination with an high-performance interior-point method (HPIPM) solver [17] for the quadratic program subproblems. The overall solving procedure is a one-click solution and is part of an automatic toolchain from IAV GmbH [18].

Figure 4 illustrates the resulting trajectories for thermal and electrical energy generation and consumption. First of all, it can be seen that the heating demand is always covered by using both the heat pump and the gas boiler. However, most of the thermal energy is generated by the heat pump due to its more economical operation. This behavior is illustrated in Figure 4a, where the gas boiler is utilized only at specific periods of high thermal demand. From Figure 4b it is particularly evident that the heat pump COP η_{HP} follows the outside temperature curve θ_{amb}. Apart from that, we can notice, that the maximum thermal power output of the gas boiler takes place during the periods of low heat pump COP.

If we take a look at the dynamics of the storage compartments' temperatures in Figure 4c, we can observe a shifting behavior, which is only possible due to the *predictive* controller. For instance, the heat storage is charged in the daytime, during the period of high heat pump COP, although no heat demand exists. For a conventional control, however, such shifting behavior would be challenging to implement, and uneconomical storage charging would take place only during the period of the peak demands.

Finally, Figure 4d illustrates the behavior of the electrical battery which is charged during the periods of high PV power generation and is discharged when the electrical power is required by the heat pump at low COP levels.

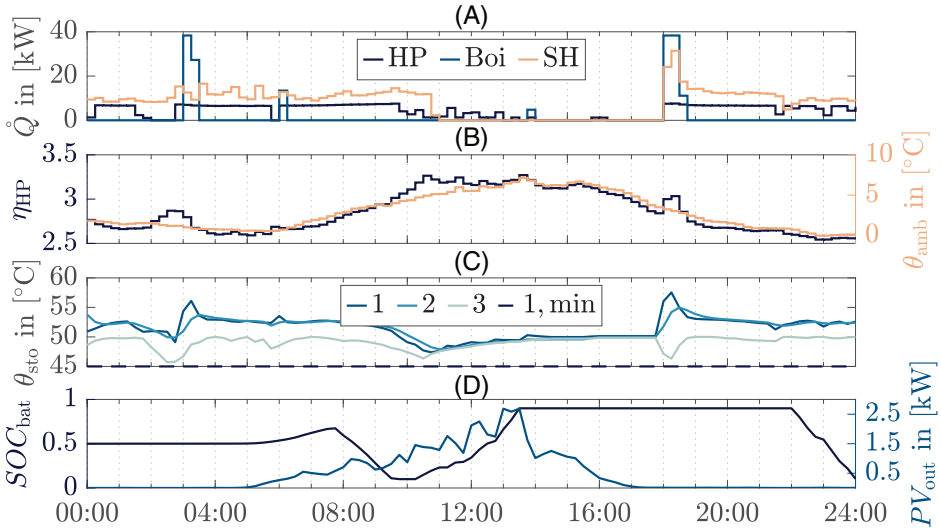

FIGURE 4 Trajectories of the power supply system. a) Thermal power output of heat pump (HP), gas boiler (Boi), and space heating demand (SH). b) Coefficient of performance of heat pump (η_{HP}) and ambient temperature (θ_{amb}). c) Temperatures of heat storage compartments (1, 2, 3) and lower bound on upper compartment (1, min). d) State of charge of battery (SOC_{bat}) and total electrical power generated by photovoltaikc system (PV_{out}).

In order for the controller to handle the rapidly changing nonlinear disturbances, we utilize a similar early-terminated SQP strategy as in [8]. It results in an average calculation time per feedback of 1.66 s with a maximum of 2.8 s on a typical laptop hardware with Intel(R) Core(TM) i7-8665U and 16.0 GB RAM. As a result, the real-time capability of the controller strategy in application to the complex system of a multifamily residential is also evident.

5 | CONCLUSIONS

A novel approach for supervisory control of building energy systems has been introduced and demonstrated through two practical case studies. The resulting optimization problem is a mixed-integer optimal control problem with specific requirements for minimum operating times, known as dwell-times. The presented strategy consists of partial outer convexification and relaxation strategies, followed by a SCARP reconstruction approach and a final post-processing step that is essential to avoid constraints' violation.

We have shown that using this approximate optimal control strategy, significant cost savings can be achieved compared to conventional control methods for a single-family home with a combined heat and power unit along with high agreement with a globally optimal solution and compliance with all system constraints. Furthermore, the applicability and real-time capability of the proposed strategy have been demonstrated for a more complex multi-family apartment complex with 18 residential units.

Future work will focus on exploring the energy and cost savings potential and the optimality of the proposed strategy for the multi-family building case, as well as its practical implementation in a real building. Also sampling time reduction and dwell-times consideration for that more complex application are parts of the forthcoming work.

ACKNOWLEDGMENTS

TUBS discloses funding by DFG (Ki 1839/1-2, Ki 1839/3-1) and by BMBF (05M20MBA-LEOPLAN). IKME is partly financed by the BMWK (03EN1007A-EEBF).

Open access funding enabled and organized by Projekt DEAL.

ORCID

Dimitri Bitner https://orcid.org/0000-0002-2528-5466

REFERENCES

1. Shaikh, P., Bin Mohd Nor, N., Nallagownden, P., Elamvazuthi, I., & Ibrahim, T. (2014). A review on optimized control systems for building energy and comfort management of smart sustainable buildings. *Renewable and Sustainable Energy Reviews*, *34*, 409–429.

2. European Commission. (2023, March 10). European Green Deal: Eu agrees stronger rules to boost energy efficiency. https://ec.europa.eu/commission/presscorner/detail/en/IP_23_1581
3. Bau, U., Baumgärtner, N., Seiler, J., Lanzerath, F., Kirches, C., & Bardow, A. (2019). Optimal operation of adsorption chillers: First implementation and experimental evaluation of a nonlinear model predictive control strategy. *Applied Thermal Engineering*, *149*, 1503–1521.
4. Bruni, G., Cordiner, S., Mulone, V., Sinisi, V., & Spagnolo, F. (2016). Energy management in a domestic microgrid by means of model predictive controllers. *Energy*, *108*, 119–131.
5. Privara, S., Široký, J., Ferkl, L., & Cigler, J. (2010). Model predictive control of a building heating system: The first experience. *Energy and Buildings*, *43*(2–3), 564–572.
6. Bürger, A., Bull, D., Sawant, P., & others. (2021). Experimental operation of a solar-driven climate system with thermal energy storages using mixed-integer nonlinear model predictive control. *Optimal Control Applications and Methods*, *42*(5), 1293–1319.
7. Bürger, A., Zeile, C., Hahn, M., Altmann-Dieses, A., Sager, S., & Diehl, M. (2020). Pycombina: An open-source tool for solving combinatorial approximation problems arising in mixed-integer optimal control. *IFAC-PapersOnLine*, *53*(2), 6502–6508.
8. Burda, A., Bitner, D., Bestehorn, F., Kirches, C., & Grotjahn, M. (2023). Mixed-integer real-time control of a building energy supply system. *IEEE Control Systems Letters*, *7*, 907–912.
9. Bitner, D., Burda, A., & Grotjahn, M. (2021). Optimized supervisory control of a combined heat and power plant by mixed-integer nonlinear model predictive control. *Proceedings of the Conference on Sustainable Energy Supply and Energy Storage Systems; NIES 2021* (pp. 1–7). IEEE, Piscataway, NJ. https://ieeexplore.ieee.org/document/9698169
10. Liberti, L. (2019). Undecidability and hardness in mixed-integer nonlinear programming. *RAIRO - Operations Research*, *53*(1), 81–109.
11. Sager, S. (2005). *Numerical methods for mixed–integer optimal control problems* [Doctoral thesis, Heidelberg University, Germany]. https://archiv.ub.uni-heidelberg.de/volltextserver/24070/1/Dissertation.pdf
12. Kirches, C. (2011). *Fast Numerical Methods for Mixed-Integer Nonlinear Model-Predictive Control*. Springer Vieweg, Berlin/Heidelberg.
13. Bock, H., & Plitt, K. (1984). A multiple shooting algorithm for direct solution of optimal control problems. *IFAC Proceedings Volumes*, *17*(2), 1603–1608.
14. Biegler, L. (1984). Solution of dynamic optimization problems by successive quadratic programming and orthogonal collocation. *Computers & Chemical Engineering*, *8*, 243–248.
15. Bestehorn, F., Hansknecht, C., Kirches, C., & Manns, P. (2019). A switching cost aware rounding method for relaxations of mixed-integer optimal control problems. *2019 IEEE 58th Conference on Decision and Control (CDC)* (pp. 7134–7139). IEEE, Piscataway, NJ.
16. Bestehorn, F., Hansknecht, C., Kirches, C., & Manns, P. (2021). Mixed-integer optimal control problems with switching costs: A shortest path approach. *Mathematical Programming*, *188*, 621–652.
17. Frison, G., & Diehl, M. (2020). HPIPM: a high-performance quadratic programming framework for model predictive control. *IFAC-PapersOnLine*, *53*(2), 6563–6569.
18. IAV | Tech Solution Provider. (2023, June 29). https://ameda.iav.com/versions.html

How to cite this article: Bitner, D., Burda, A., Grotjahn, M., Kirches, C., Schild, A., & Luck, B. (2023). Mixed-integer NMPC for real-time supervisory energy management control in residential buildings. *Proceedings in Applied Mathematics and Mechanics*, *23,* e202300219. https://doi.org/10.1002/pamm.202300219